# POTENTIAL INDUCED DEGRADATION EFFECT ON N-TYPE SOLAR CELLS WITH BORON EMITTER

**Barbora Mojrová**

Doctoral Degree Programme (4), FEEC BUT

E-mail: xmojro00@stud.feec.vutbr.cz

Supervised by: Jaroslav Boušek

E-mail: bousek@feec.vutbr.cz

**Abstract**: This study is focusing on Potential Induced Degradation (PID) effect on *n*-type solar cells with boron emitter. We designed and fabricated single cell modules using *n*-PERT cells with textured and flat front side, and with various passivation structures on the front side to prevent PID at the cell level. The modules were characterized before and after PID testing by electroluminescence (EL), IV measurements, reflection and Internal Quantum Efficiency (IQE). Measurements were done on both sides of module to obtain whether the degradation was going on the front side, rear side or both. Comparison of IQE of front vs rear side shows, that intensity of degradation is fully influenced by properties of the front side of antireflection and passivation (ARC) layer.

**Keywords**: PID, *n*-type, solar cell, passivation layer, boron emitter

## 1 INTRODUCTION

The potential induced degradation is an undesirable property of solar cell modules. PID occurs in the photovoltaics systems due to high voltage stress across the module layer stack between framing/glass surface and solar cells and leads to significant power losses. These high voltages may cause leakage current between the solar cells and the module frame through the front glass and encapsulation, being responsible for degradation effects [1].

The choice of glass, encapsulation, and diffusion barriers has been shown to have an impact on PID on the module level [2-4]. On the cell level properties of the antireflection and passivation layer (ARC) have also impact on the PID. PID in *n*-type Si modules is caused by enhanced front surface recombination [5, 6]. The goal of this study is to find a passivation structure to prevent degradation already at the cell level for n-type solar cells.

## 2 SAMPLE PREPARATION

In this work we investigated the influence of different composition of ARC layer on PID at *n*-PERT cell concept with front boron emitter and a phosphorous back surface field (BSF) with screen printed and fired through metallization of commercial silver (Ag) paste on both sides. A schematic cross-section of the studied solar cells is presented in the Fig. 1.

For experiment we used 6 inch *n*-type (phosphorous doped) monocrystalline Si wafers (239 $cm^2$). The base resistivity $\rho_{base} = 2 - 3\ \Omega cm$. Wafers were processed using standard industrial process, which includes wet chemical alkaline texturization, diffusion in quartz tube furnace containing $POCl_3$ ($n^+$ BSF, resulting sheet resistance of 65 Ω/sq) or $BBr_3$ ($p^+$ emitter, resulting sheet resistance of 75 Ω/sq), deposition of ARC layer, screen printing of Ag finger grid on both sides, and co-firing. The half of samples had textured front side, the rest of them had flat front side.

In this experiment we tested 7 different compositions of ARC layer, named G1 – G7 (see the Tab. 1). For groups G1 – G4 the 10 nm thick layer of thermal $SiO_X$ was deposited on boron emitter, then PECVD $SiN_X$ layer with different refractive index followed, and in case of G4 samples the PECVD $SiO_X$ was deposited at last. For samples from groups G6 – G7 the 1.5 nm thin layer of $SiO_2$ was formed by the Nitric Acid Oxidation of Silicon (NAOS) method and then the PECVD $SiN_X/SiO_X$ layers were deposited.

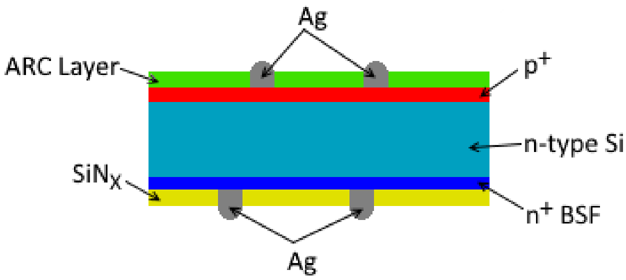


**Figure 1:** Schematic cross-section of the investigated *n*-PERT cells.

**Table 1**: The overview of investigated ARC layers.

| | G1 | G2 | G3 | G4 | G5 | G6 | G7 |
|---|---|---|---|---|---|---|---|
| Emitter | $p^+$ | $p^+$ | $p^+$ | $p^+$ | $p^+$ | $p^+$ | $p^+$ |
| 1st layer | $SiO_X$ (10 nm) | $SiO_X$ (10 nm) | $SiO_X$ (10 nm) | $SiO_X$ (10 nm) | $SiO_X$ (30 nm) | NAOS (1.5 nm) | NAOS (1.5 nm) |
| 2nd layer | $SiN_X$ (n = 2.05) | $SiN_X$ (n = 2.08) | $SiN_X$ (n = 2.22) | $SiN_X$ (n = 2.22) | $SiN_X$ (n = 2.05) | $SiN_X$ (n = 2.05) | $SiO_X$ (100 nm) |
| 3rd layer | - | - | - | $SiO_X$ (100 nm) | - | - | $SiN_X$ (n = 2.05) |

Full-size 3 busbar single cell mini-modules were fabricated using solar cover glass, ethylene-vinyl acetate copolymer (EVA) for the encapsulation, and standard transparent back sheet material. The structure of module is given in the Fig. 2.

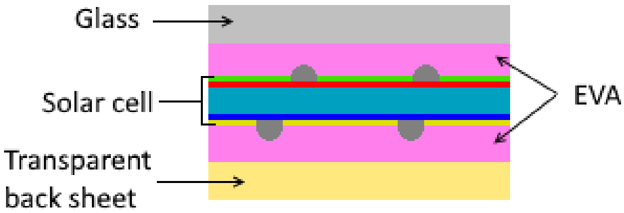


**Figure 2:** Schematic cross-section of the investigated module.

## 3 RESULTS

Completed solar cells were investigated by IV measurements to determine the values of short-circuit current ($J_{SC}$) and $V_{OC}$ on the cell level. The modules were characterized before and after PID testing by EL, IV measurements, reflection and IQE. Measurements were done on both sides of module to obtain whether the degradation was going on the front side, rear side or both. The PID tests were performed by applying high voltage (-1000 V) to modules for 23 or 46 h. The modules were placed with the glass side facing down on the metal base plate. An aluminium foil between the plate and the module front side simulates the module frame and guarantees proper contacting.

### 3.1 IV MEASUREMENT

IV measurements of modules were done before and after PID testing to determine changes in $J_{SC}$, $V_{OC}$, fill factor (FF) and pseudo fill factor (pFF). The origin of the power drop at PID effect is a decrease of $J_{SC}$ (which is shown in the Fig. 3) and $V_{OC}$. Fill factor and pseudo fill factor stay nearly constant for all samples which indicates that PID does not cause cell shunting in our case.

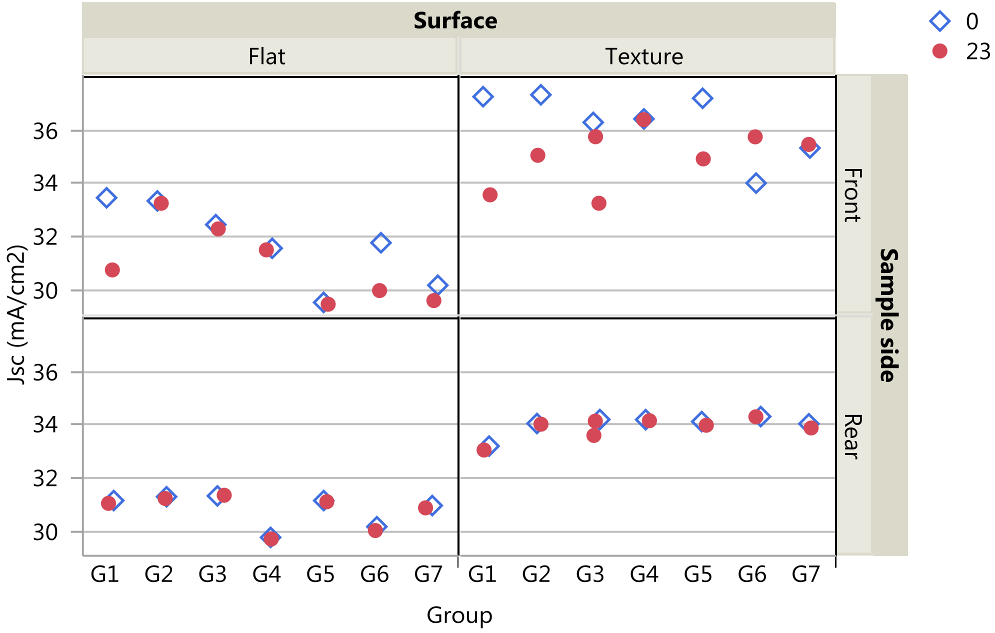


**Figure 3:** Comparison of $J_{SC}$ before and after PID test.

### 3.2 EL MEASUREMENT

The EL measurements were done to get an impression of the behaviour of investigated *n*-PERT cells under PID stress. The Fig. 4 shows examples of EL images for the mini-module before and after the PID test. The EL reveals localized defects of the module after PID state where lower signal means that the non-radiative recombination in the solar cell has increased. This is another hint that the power drop stems from a loss of front surface passivation.

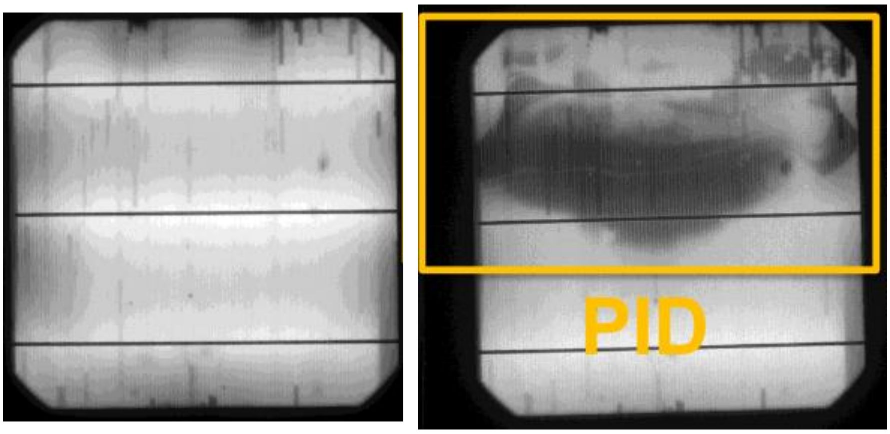


a) before degradation b) after 23 h degradation

**Figure 4:** EL picture of sample G2 with textured surface in the initial state (a) and after 23 h degradation(b).

### 3.3 IQE MEASUREMENT

Comparison of the IQE of front versus the rear side (see Fig. 5) indicate that degradation process is related to a degradation of the front side of solar cell. The type of texturization has no significant influence on degradation.

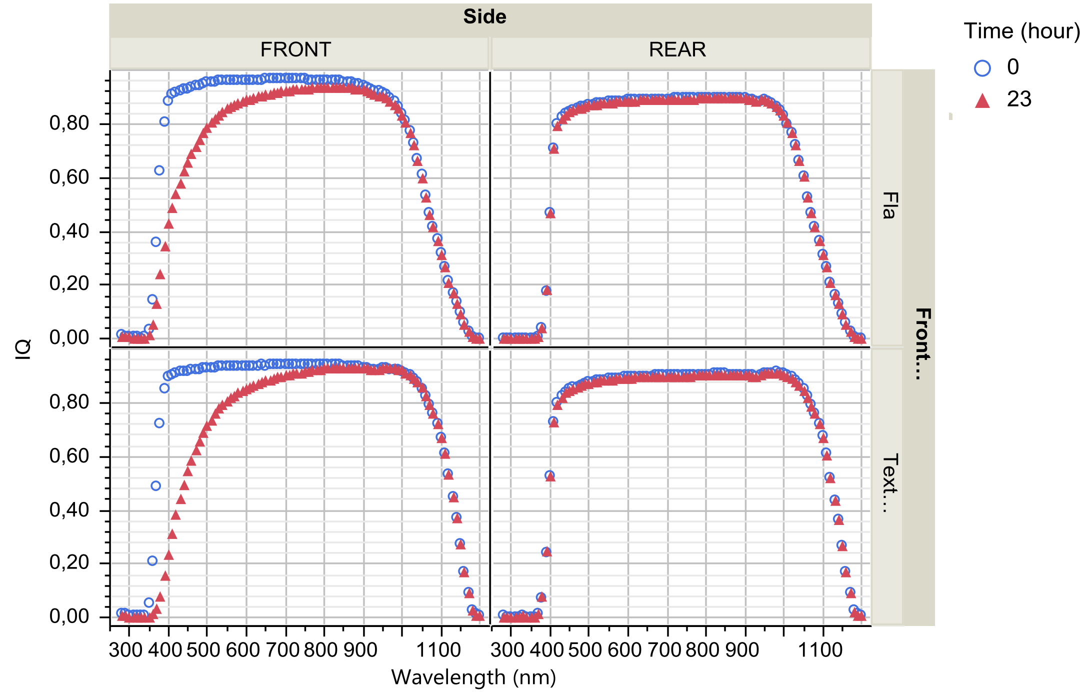


**Figure 5:** Calculated IQE for front/rear side of samples from G1 with flat/textured front side before and after degradation.

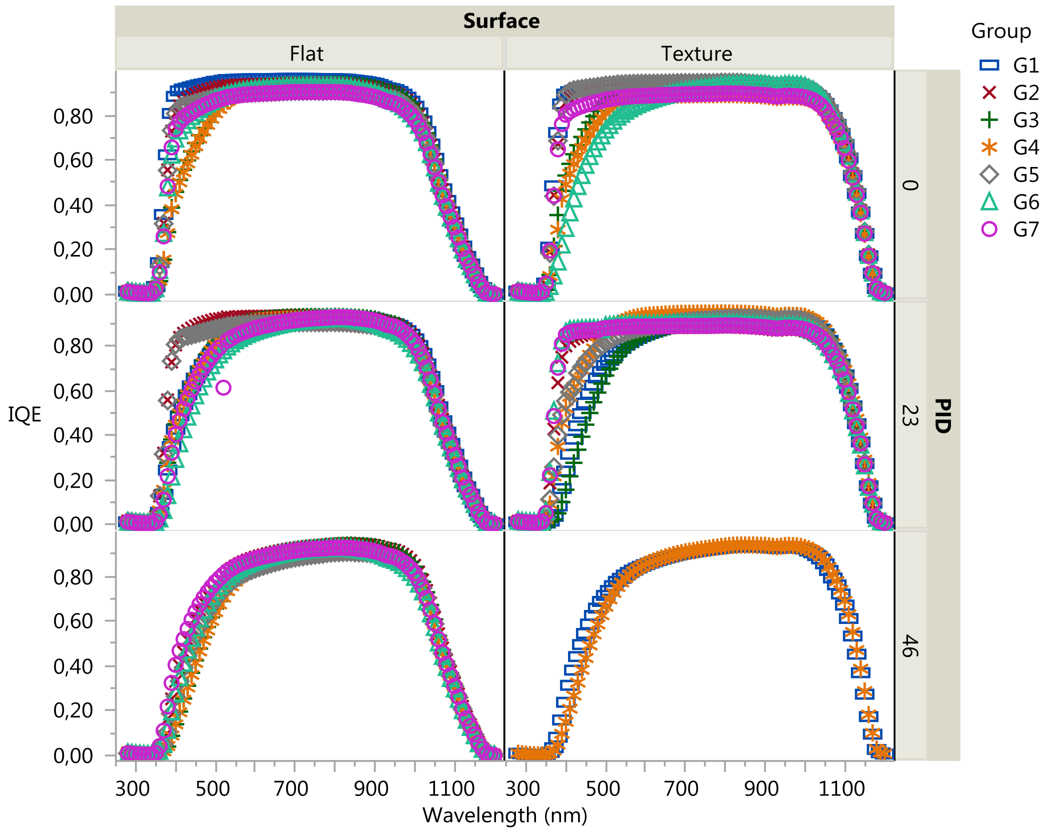


**Figure 6:** Calculated IQE for front side of solar cells before and after 23 or 46 h degradation.

The IQE decreased in the range from 400 nm to 700 – 800 nm (see Fig. 6), although no change was observed from 800 to 1100 nm. This could be caused by increase of the value of front surface recombination velocity which leads to decrease of spectral response in the short-wavelength region (λ < 500 nm). Short-wavelength photons are absorbed in the heavily doped part of emitter. Therefore the change of IQE spectrum could be caused by the enhanced front surface recombination.

## 4 CONCLUSION

In this experiment we observed a power degradation mechanism for encapsulated *n*-type PERT cells with boron emitter after applying a negative voltage stress between encapsulated solar cell and a metal plate covered with Al foil. Different ARC layers deposited on flat/textured emitter were tested while no significant differences were observed, because all structures showed degradation after 23 or 46 h.

The severe $J_{SC}$ degradation measured in experiments suggests an additional effect, e.g. a decrease of the diffusion length in the emitter due to contamination by in-diffused ions. More detailed characterization is needed to identify the root cause of the degradation mechanism we observed. The EL images have revealed the position of PID defects. The lower signal was caused by increasing of non-radiative recombination in the solar cell.

From IQE results it is obvious that the degradation process is related to a degradation of the front side ARC layer, where the boron emitter is present and it is caused by the enhanced front surface recombination. Type of texturization has no significant influence on degradation on the front side.


## ACKNOWLEDGEMENT

The article was supported by project no. FEKT-S-17-3934, Utilization of novel findings in micro and nanotechnologies for complex electronic circuits and sensor applications.


## REFERENCES


[1] Bauer, J., V. Naumann, S. Großer, et al. On the mechanism of potential-induced degradation in crystalline silicon solar cells. *Physica status solidi (RRL) - Rapid Research Letters* [online]. 2012, 6(8), 331-333 [cit. 2017-03-14]. DOI: 10.1002/pssr.201206276. ISSN 18626254

[2] Halm, A., A. Schneider, V. D. Mihailetchi, et al. Potential-induced Degradation for Encapsulated n-type IBC Solar Cells with Front Floating Emitter. *Energy Procedia* [online]. 2015, 77, 356-363 [cit. 2017-03-14]. DOI: 10.1016/j.egypro.2015.07.050. ISSN 18766102.

[3] Pingel, S., O. Frank, M. Winkler, et al. Potential Induced Degradation of solar cells and panels. In: *2010 35th IEEE Photovoltaic Specialists Conference* [online]. IEEE, 2010, s. 002817-002822 [cit. 2017-03-14]. DOI: 10.1109/PVSC.2010.5616823. ISBN 978-1-4244-5890-5.

[4] Naumann, V., T. Geppert, S. Großer, et al. Potential-induced Degradation at Interdigitated Back Contact Solar Cells. *Energy Procedia* [online]. 2014, 55, 498-503 [cit. 2017-03-14]. DOI: 10.1016/j.egypro.2014.08.015. ISSN 18766102

[5] Stodolny, M. K., G. J.M. Janssen, B. B. Van Aken, et al. PID- and UVID-free n-type Solar Cells and Modules. *Energy Procedia* [online]. 2016, 92, 609-616 [cit. 2017-03-14]. DOI: 10.1016/j.egypro.2016.07.026. ISSN 18766102.

[6] Hara, K., S. Jonai and A. Masuda. Potential-induced degradation in photovoltaic modules based on n-type single crystalline Si solar cells. *Solar Energy Materials and Solar Cells* [online]. 2015, 140, 361-365 [cit. 2017-03-15]. DOI: 10.1016/j.solmat.2015.04.037. ISSN 09270248.